Available online at www.sciencedirect.com

ScienceDirect

Procedia Structural Integrity 18 (2019) 875–885

Structural Integrity Procedia

www.elsevier.com/locate/procedia

25th International Conference on Fracture and Structural Integrity

Evaluation of the heat dissipated around the crack tip of AISI 422 and CF3M steels by means of thermography

Palumbo Davide*, De Finis Rosa, Galietti Umberto

Politecnico di Bari, Department of Mechanics, Matematics and Management (DMMM), Viale Japigia 182, 70126, Bari, Italy

Abstract

The fatigue crack growth depends on the dissipated energy at the crack tip and in this regard, different analytical and numerical models were proposed by many researchers to describe as the plastic work affect the fatigue material behaviour. Experimental tests can be carried out for evaluating the energy dissipated during the crack growth principally based on the hysteresis loop measurement. However, these techniques need of suitable equipment and set-ups and then find some restrictions if applied in-situ and on real components.

In this work, an experimental approach is used to obtain a thermographic parameter capable of describing the plastic work at the crack tip. The proposed approach is based on the phase shift of the thermal signal that occurs at the crack tip in the plastic area.

Two specimens of two different steels, austenitic and martensitic, were tested and monitored with an infrared camera to collect thermoelastic phase data. A similar correlation to the dissipated energy was obtained with the fatigue crack growth behavior of materials.

Peer-review under responsibility of the Gruppo Italiano Frattura (IGF) ExCo.

Keywords: Dissipated energy; thermoelastic signal; phase signal; crack growth; steels.

* Corresponding author. Tel.: +39 3495990841

E-mail address: davide.palumbo@poliba.it

2452-3216
Peer-review under responsibility of the Gruppo Italiano Frattura (IGF) ExCo.
10.1016/j.prostr.2019.08.238

1. Introduction

The fatigue crack growth depends on many factors related to the material and the micro-mechanisms that act at the crack tip. Paris and Erdogan (1963) firstly described the crack growth rate behavior as a function of the stress intensity factor (SIF) (1999). In particular, this latter and the crack growth are related through two constants of material that can be obtained by means of experimental tests according to Standards (2004).

In the last years, many researchers focused their attention on energy-based approaches (Weertman, 1973; Klingbeil, 2003; Mazari et al., 2008; Kucharski et al., 2016; Ranganathan et al., 2008). Indeed, the dissipated energy plays a key role in the crack growth behavior and can be used to describe the plastic work at the crack tip. The energy-based approach, proposed firstly by Weertman (1973), links the crack growth rate with the critical energy to create a unit surface area. Similar results were obtained by Klingbeil (2003), where the crack growth in ductile solids is governed by the total cyclic plastic dissipation ahead of the crack. Mazari et al. (2008) starting from the Weertman's and Klingbeil's approach, developed a new model in which a similar Paris Law model was obtained between the crack growth and the heat dissipated per cycle.

Different experimental approaches were used in literature focused on determining the critical energy by means of strain gages in the plastic zone, Ranganathan et al., (2008), calorimetric measurements, Ikeda et al., (1977) and hysteresis loop evaluation, Mazari et al., (2008). More recently, thermographic techniques were used aiming to determine the heat sources at the crack tip in the cyclic plastic zone (Carrascal et al., 2014; Cui et al., 2015; Meneghetti et al., 2016; Ancona et al., 2016; Palumbo et al., 2017).

Infrared Thermography (IRT) is a full-field contactless technique used in many fields such as, non-destructive testing (NDT), process monitoring and evaluation of heat sources during fatigue tests. In particular, many approaches are present in literature in which the IRT technique is used for investigating the fatigue behaviour of steels (Meneghetti, 2007; Palumbo et al., 2017; De Finis et al., 2019). Less works regards the monitoring of the fatigue crack growth. In particular, a temperature rise due to the heat dissipations can be observed around the crack tip where the plastic zone is located. In this regard, Carrascal et al., (2014) used IRT for evaluating the Paris Law constants of a polymer (polyamide) with an experimental methodology. A good agreement was found with respect to traditional calculation methods. Cui et al. (2015), applied IRT to study the fatigue crack growth of magnesium alloy joints and demonstrated the potential of IRT in predicting the threshold value for unstable crack growth.

In the work of Meneghetti et al. (2016), experimental tests were performed for evaluating from temperature measurements the specific heat energy per cycle averaged in a small volume surrounding the crack tip.

The above exposed procedures are based on temperature data and can find limitations in some applications in which the temperature changes due to the plastic work are very low. This is the case of brittle or materials with high diffusivity. In this regard, Palumbo et al. (2017) presented a new procedure based on the processing of thermographic signal in the frequency domain. In particular, the harmonic of the temperature signal at the twice of the loading frequency has been used to estimate the heat dissipated at the plastic area.

Interesting results in assessment of plastic zone and SIF were obtained by using the Thermoelastic Stress Analysis (TSA) (Dulieu-Barton, 1999; Pitarresi et al., 2003; Wang et al., 2010; Harwood et al., 1991; Stanley, 1997; Dunn, 1997; Dulieu-Smith, 1995). By knowing the sum of the principal stresses, it is possible to determine the stress intensity factor, and at the same time, it is possible to determine the crack growth rate by analyzing the phase data (Tomlinson et al. 1999; Tomlinson et al., 2011; Diaz et al., 2004; Diaz et al., 2004). In this regard, Ancona et al. (2015, 2016) proposed an automatic procedure based on TSA, to assess the Paris Law constants and to study the fracture behaviour of 4 stainless steels.

In this work, the thermoelastic phase signal has been used as an index for monitoring the energy dissipated at the crack tip and then the fatigue crack growth behaviour of two steels: AISI 422 and CF3M.

Two CT steel specimens were used and tested according to ASTM E 647-00 and the monitoring of crack tip growth was performed in a continuous manner by means of a cooled IR camera. Thermal data were processed in the frequency domain in order to extract the thermoelastic phase signal related to the energy dissipated at the crack tip. Similar relations were obtained between the crack growth, the phase signal and the energy dissipated per cycle and the capability of the phase signal in describing the fatigue crack growth has been demonstrated.

2. Theory

In absence of material phase transitions, the response of a material to a mechanical cyclic excitation, in presence of dissipative intrinsic processes involves a hysteresis loop due to phenomena producing energy dissipations. Considering a cyclic test, in load control, these phenomena determine a retardation of the strain with respect to the imposed stress, here indicated as 'ψ', Figure 1a, De Finis et al., (2019).

For assessing and quantifying the energy of internal friction, viscoelasticity and micro-plasticity one can refer to dumping phenomena (). A common procedure involves the study of the area under a generic hysteresis loop.

In Figure 1b, is depicted a hysteresis loop at the most general loading ratio to which all the cases can be referred (R=-1), in presence of non-adiabatic deformation process, the figure also reports the completely elastic behaviour of the materials which is represented by the line k-h.

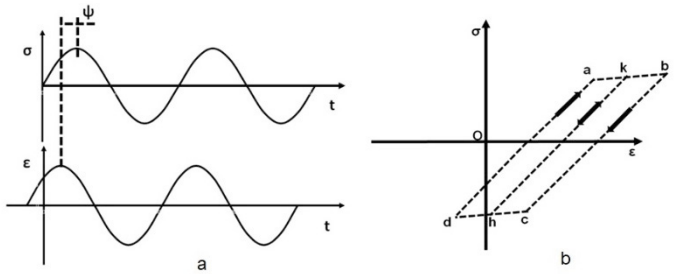

Fig. 1. Phase shift between strain and stress during (a) fatigue loading and (b) a generic hysteresis loop, De Finis et al., (2019).

Although the test is running at a stress ratio different from -1, generally, the onset of damage phenomena leads to a local change of stress ratio, so that certain zones of the material may undergo tension-compression conditions due to the plasticisation. For this reason, in presence of damage, it is possible to refer to the case of full-inversion conditions (R=-1) as the most general case.

The model of figure 1b, however, disregards some aspects related to kinematic and isotropic hardening47. In these conditions, in fact, the study of the viscos-plastic behaviour is described by a simple relation between stress and strain and the energy of dissipative processes can be somehow quantified by calculating the area of hysteresis loop (Ap) which is, in turn, related to the phase shift between strain and stress, 'ψ'.

By focusing the attention on the energy involved in the process, the dissipative phenomena (e.g. viscous or plastic phenomena) occurring in the lattice in a fixed finite continuous volume of an isotropic and homogenous material 'V_p', can be described by using the first principle of thermodynamics, De Finis et al., (2019):

$$W_p = \Delta U + Q = Q + E_p + E_d \tag{1}$$

where 'Wp' is the supplied mechanical energy, ΔU' is the internal energy per cycle variation due to microstructural rearrangements, to the formation of persistent slip bands and to all the phenomena related to irreversible dislocation movement in the lattice. A portion of this energy does not remain under mechanical form but converts into heating, in particular, it contributes to the irreversible heat source development in the material and, furthermore, it affects the temperature growth. The term 'Q' represents the heat exchanges (radiation, conduction, convection) which may be totally ascribed to heat conduction between the regions of the sample. The term 'Ep' refers to the mechanical work introduced in the material system during the plastic phenomena that is a portion of internal energy 'ΔU'. As said before, it is correlated to irreversible changes of shape of the material. 'Ed' is the energy per cycle dissipated as heat. It includes the irreversible dissipative phenomena generated by the intrinsic heat sources (related to plastic phenomena) or internal energy variation (related to viscous phenomena) producing thermal effects De Finis et al., (2019).

Different energetic contributions due to specific physical phenomena such as micro-plasticity, micro-friction taking place inside the material will determine a characteristic temperature evolution with time generating a specific thermal signature according to the specific phenomenon.

The heat production, however, becomes significant when the load increases and so this heat generation itself in the analyzed volume, determines the loss of adiabatic conditions, in fact, in presence of heat exchanges ($Q \neq 0$), the temperature increases until a steady state value is reached De Finis et al., (2019).

The total temperature variation includes all the temperature variations related to both irreversible and reversible heat dissipations.

The temperature variations from irreversible processes vary with twice the mechanical frequency since they are related to the linear increasing of energy that is found to be twice per cycle in the material while as widely discussed in literature, the reversible temperature variations are due to the volume variations.

However, in Equation 1, thermoelastic source is not present because of its reversible nature, which provides a null contribution in one cycle.

In the case of uniaxial stress with sinusoidal loading, the relative temperature variations can be expressed in frequency domain as follows De Finis et al., (2019):

$$T = T_{the}\, sin(\, 2\pi f t + \pi + \phi) \tag{2}$$

where 'T' are the temperature variations running at the mechanical exciting frequency 'f', 'Tthe' is the amplitude of the signal and 'φ' is the phase angle between temperature and loading signal. The symbol 'π' has been included according to the classic theory of thermoelastic stress analysis, where the temperature and first stress invariant have opposite signs.

Two main cases can be represented to explain how different processes contribute to temperature retardation with respect to the stress: elastic regime and viscos-plastic regime, as represented in Figure 2.

Under adiabatic conditions, in case of perfect linear elastic behaviour, the stress and strain are supposed to be in phase and 'T' the thermoelastic temperature variations are out-of-phase of a fixed quantity 'π' (positive sign of the first stress invariant of Equation 2) De Finis et al., (2019), Figure 2a.

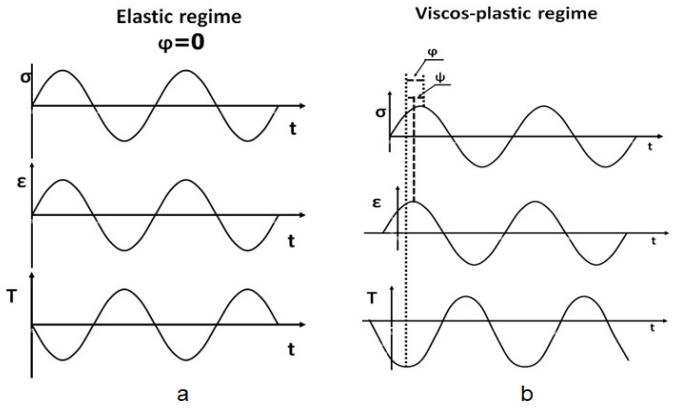

Fig. 2. Graphical representation of phase shifts between stress-strain and temperature: (a) elastic conditions and (b) viscos-plastic behavior, De Finis et al., (2019).

In Figure 2a, the energy variations related to thermoelastic temperature variations are zeros in a cycle, hence no temperature increase and accumulation in the material is present.

Under viscos-plastic regime, the atoms movements produce a retardation of the material response to such the excitation, that determine the phase shift between stress and strain, 'ψ', as said before, Figure 2b.

In these conditions, the equation 1 is valid and the intrinsic frictions (reversible and irreversible atoms movement) occurring in the crystal lattice, produce heat.

The heating produced into the lattice leads to a temperature increase and conduction heat exchanges, which in turns affects the adiabatic conditions. In general, the presence of intrinsic heat source or thermal heat exchanges determine a temperature retardation with respect to the reference signal, that is the imposed stress. Hence, the phase shift 'φ' assumes a value different from zero.

The phase shifts 'φ' and 'ψ' are strict related. The thermoelastic phase assessed using equation 2 represents an index of energy and heat involved in hysteresis processes with dissipative heat sources. However, in the aim of the present paper there is not the separation or the determination of each one or both 'φ' and 'ψ', this paper is aimed to understand the physic of the processes that determine the presence of 'φ', the phase shift related non-adiabatic process.

So that, the phase shift can be generally indicated.

It is important to highlight as the 'φ' assessment depends also on external factors that could affect its measurement, such as:

-non-perfect homogeneity of surface coating

-geometric surface imperfections

-electronic noise of hardware.

In following sections, materials and methods will be described and the results obtained in terms of phase signal at in the plastic area for two different steels will be discussed.

3. Experimental set-up

3.1. Specimens geometry and materials

The tested materials are the martensitic steel AISI 422 and the austenitic one CF3M. Martensitic stainless steels have a higher mechanical strength obtained by a quenching heat treatment compared with austenitic steels; the corrosion resistance is higher in austenitic stainless steel due to the higher percentage of chromium. In Tables 1 and 2, the chemical composition and the mechanical properties of the stainless steel tested in this work are presented, Tomei (1981).

Table 1. Chemical composition of stainless steels tested in the work.

Materials [%]	**C**	**P**	**Si**	**Ni**	**V**	**Mn**	**Cr**	**S**	**Mo**	**W**
AISI 422	0.20-0.25	0.025	0.4	0.50-1.00	0.15-0.30	1.0	11.0-13.0	0.025	0.75-1.25	0.75-1.25
CF3M	0.03	0.015	1.0	10.0-14.0	-	2.0	10.0-18.0	0.030	2.00-3.00	-

Table 2. Mechanical properties (at room temperature).

Materials	**E** [MPa]	σ_y [MPa]	σ_{UTS} [MPa]
AISI 422	200,000	760	966
CF3M	200,000	276	586

Three Compact Tension (CT) specimens were used with dimensions according to ASTM E 647 (2004). In Figure 3 dimensions of the specimen are reported in mm. Specimens were sprayed with flat black spray for increasing the emissivity to 0.95.

3.2. Testing procedure

The tests were carried out with the MTS model 370 servo hydraulic fatigue machine with a 100 kN capacity. According to ASTM E 647 (2004) the constant-force-amplitude procedure was used with a constant force range of ΔP=10.8 kN for AISI 422 and ΔP=9.9 kN for CF3M. Moreover, a fixed stress ratio (R=0.1) and loading frequency f=13 Hz were adopted.

Thermographic sequences were acquired with constant intervals of 2,000 cycles by using a cooled FLIR IR X6540 SC infrared camera with an InSb detector (640x512 pixels) and acquisition rate of 123 Hz, Figure 4. A geometrical resolution of 0.067 mm/pixel was obtained placing the thermocamera at 170 mm from the specimen and by using a 50 mm lens with a 12 mm extension ring. All specimens were pre-cracked until to reaching a crack length of 2.5 mm according to ASTM E-647.

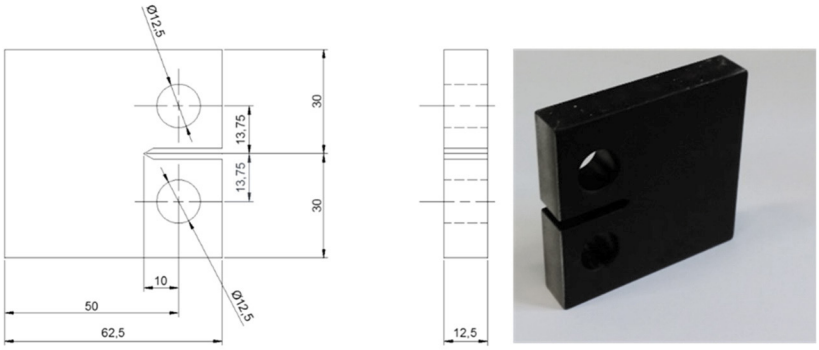

Fig. 3. Specimen dimension in mm according to ASTM E 647.

Fig. 4. Experimental set-up used for testing.

4. Methods and data analysis

Acquisition systems used in TSA are usually based on a correlation in frequency, amplitude and phase of the detected signal with a reference signal coming from the loading system. TSA analysis provides a S signal proportional to the peak-to-peak variation in temperature during the peak-to-peak variation of the sum of principal stress. S is usually presented as a vector, where modulus is proportional to the change in temperature due to the thermoelastic effect and the phase φ means the angular shift between the thermoelastic and the reference signal, Diaz et al., (2004).

In order to respect the adiabatic conditions, TSA is usually performed by applying a sinusoidal loading to material with a suitable loading frequency (). In this case, the generic measured uncalibrated thermographic signal s can be represented in the time domain as follows:

$$s = \frac{1}{A}\sigma_a \, sin(\omega t + \pi + \phi) = \frac{S}{2} sin(\omega t + \pi + \phi) \tag{3}$$

where ω is the frequency loading, A is a calibration constant, σ_a is the stress semi-amplitude and φ is the phase angle between thermoelastic and loading signal.

Referring to equation 3, a mathematical algorithm implemented in IRTA® software (2015) has been used to extract pixel by pixel phase angle and the amplitude S of the thermoelastic signal. In particular, a suited signal model has been used, as indicated in equation 4:

$$s = b_1 + b_2 \sin(\omega t + \varphi') \tag{4}$$

where the term b1 represents the mean temperature rise, b2=S/2, and $\varphi'=\pi+\varphi$.

The proposed procedure can be summarized as follows:

- Thermographic sequence acquisition with infrared camera;
  Thermal sequences of about 10 seconds have been acquired at regular intervals of 2000 cycles during the test.

- Thermoelastic phase data assessing;
  About 2 minutes are required to extract the TSA data (phase data) from each thermal sequence by means of the IRTA software.

- Extraction of the analysis area from the phase images in order to obtain the phase data matrix;

- Shifting of the selected phase data in order to report the average phase data to zero away from crack tip.
  This operation is obtained by subtracting the average value of phase signal taken away from the crack tip, to the all phase data;

- Evaluation of the minimum value of phase signal in the selected area of analysis;

5. Results and discussion

In this section, the results in terms of phase maps and phase data will be presented and a comparison between the two analysed stainless steels will be shown. As exposed in the previous section, phase data have been obtained by processing thermal sequences acquired each 2000 cycles.

Figures 5 and 6 show the phase maps in correspondence of four different values of number of cycles for the two steels. It is clear as the AISI 422 presents a regular crack growth with respect to the CF3M that show changes in crack growth direction. This it is simply explained by considering the different mechanical behavior of the two steels, a brittle behavior for the AISI 422 with respect to the ductile behavior of CF3M. In the both phase maps, the typical phase signal at the crack tip is observed, Ancona et al, (2016), characterized by a change in sign along the crack growth direction. In particular, a delay of the phase signal is present ahead the crack tip. Indeed, in an area around the crack tip, plastic conditions are reached, due to the high stress values that exceed the yield stress of material. As it shown in the theory section, in this area, a mechanical energy is dissipated due to the plastic work, and the phase value can be considered as an index of this energy. Part of this energy is dissipated as heat. The heat source induces the loss of adiabatic conditions (heat diffusion in-plane and in-depth) and then a positive phase shift just beyond the plastic area.

In this work the attention was focused on the value of the phase signal in the plastic area (negative value). Figure 7 show for the two material the value of the phase as function of the number of cycles. It is worth to notice as, for simplicity, the phase values are represented as positive. It is very interesting to notice as the phase trend and in particular, the phase increasing, seems very similar to the crack growth rate. Another interesting result is obtained if the phase values are represented with respect to the SIF, Figure 8a. Indeed, a good linear relation (in a double log scale) between the phase and SIF is obtained in agreement with the energy approach proposed by Weertman (1973).

The SIF values were evaluated according to the Standard ASTM E 647 (2004) and the following equation:

$$\Delta K_I = \frac{\Delta P}{B\sqrt{W}} \frac{(2+\beta)}{(1-\beta)^{3/2}} (0.886 + 4.64\beta - 13.32\beta^2 + 14.72\beta^3 - 5.6\beta^4) \quad (5)$$

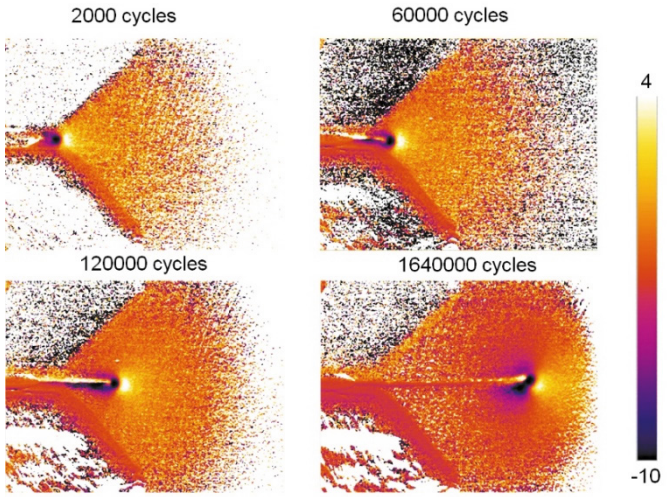

Fig. 5. Phase maps and crack evolution for different values of the number of cycles (AISI 422)

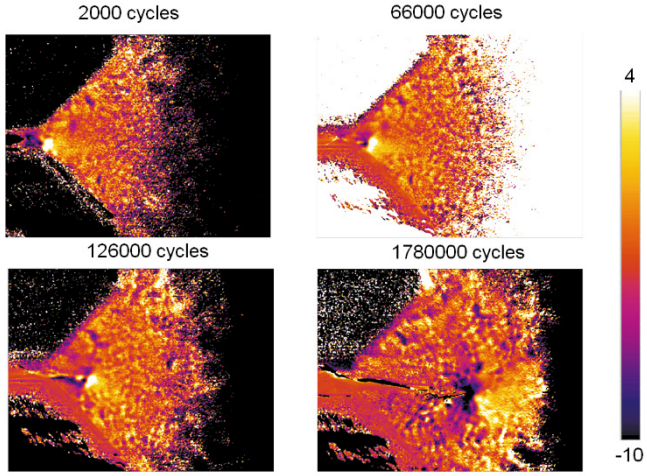

Fig. 6. Phase maps and crack evolution for different values of the number of cycles (CF3M)

Figure 8b, shows the evolution of crack growth rate with respect to the phase values for the two materials. Also, in this case, a linear relation can be determined between these two parameters:

$$\frac{da}{dN} = b\Delta\varphi^c \quad (6)$$

A similar relation has been determined and verified by other authors by considering the dissipated hysteretic energy per cycle, Kucharski et al. (2016). These results demonstrate as eq. 6 can be used for evaluating the crack growth rate by knowing the heat dissipated per cycle ahead of the crack tip. In particular, in very similar way to the Paris Law, the fatigue crack growth can be described by the phase signal. In Figure 9 are shown the results obtained with the

crack growth rate measured by means of TSA, Ancona et al., (2016). In particular, in Ancona et al., (2016), the phase of thermoelastic signal has been used to estimate the crack tip position over time and the procedure has been validated by comparison with optical measurement.

Also, in this case, it is interesting to notice as the phase signal is capable to discern the different fatigue crack growth behavior as well as the classical Paris Law data.

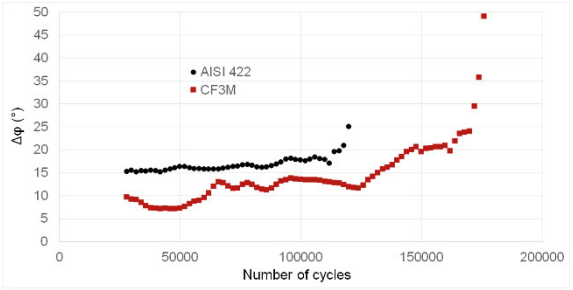

Fig. 7. Phase signal as a function of the number of cycles.

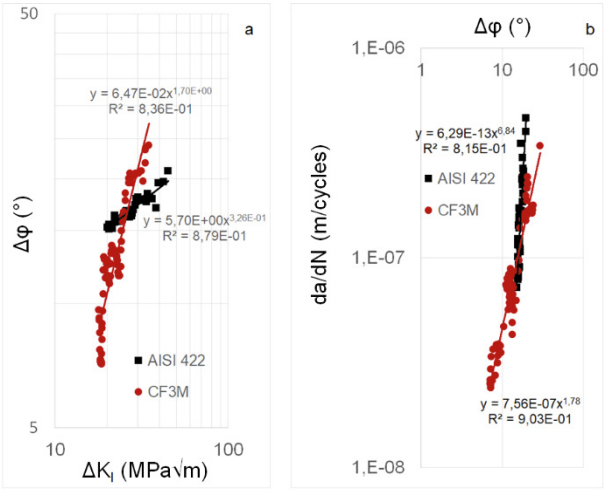

Fig. 8. Phase signal as a function of the SIF (a) and crack growth rate as a funtion of the phase signal.

6. Conclusions

In this work, the phase signal has been used to describe the fatigue crack growth in two steels AISI 422 and CF3M

Two CT specimens were tested and monitored by means of a cooled infrared camera in order to acquire thermographic sequences during tests at regular intervals (2,000 cycles each).

The proposed approach uses the analysis of the thermal signal in the frequency domain in order to extract the phase signal related to the energy dissipated at the crack tip.

The main results can be summarized as follows:

- a similar Paris Law model was obtained between the crack growth rate and the phase signal,
- it was obtained a good correlation between the phase signal and the Stress Intensity Factor in agreement with numerical and analytical models present in literature that consider the energy dissipated in place of the phase signal,
- the phase signal seems to discern in significant way the different fatigue crack growth behavior of the two steels.

Finally, it is worth to underlining as the proposed method can also be used for the monitoring of damage or crack growth within real and more complex structures subjected to actual loading conditions

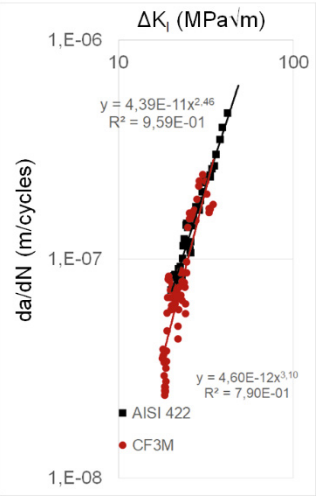

Fig. 9. Paris Law for AISI 422 and Cf3M obtained in, Ancona et al. (2016)

References

Paris, P., Erdogan, F., 1963. A critical analysis of crack propagation laws. Journal of Basic Engineering, Transactions of the American Society of Mechanical Engineers D 85(4), 528-534, DOI: 10.1115/1.3656900.

Ritchie, R.O., 1999. Mechanisms of fatigue-crack propagation in ductile and brittle solids. International Journal of Fracture 100, 55-83.

ASTM E 647-00: Standard Test Method for Measurement of Fatigue Crack Growth Rates, 2004.

Weertman, J., 1973. Theory of fatigue crack growth based on a BCS crack theory with work hardening. International Journal of Fatigue 9, 125-155.

Klingbeil, N.W., 2003. A total dissipated energy theory of fatigue crack growth in ductile solids. International Journal of Fatigue 25(2), 117-128.

Mazari, M., Bouchouicha, B., Zemri, M., Benguediab, M., Ranganathan, N., 2008. Computational Materials Science 41, 344-349.

Kucharski, P., Lesiuk, G., Szata, M., 2016. Description of Fatigue Crack Growth in Steel Structural Components Using Energy Approach – Influence of the Microstructure on the FCGR. In: Fatigue failure and fracture mechanics XXVI: proceedings of the XXVI Polish National Conference on Fatigue Failure and Fracture Mechanics, (Dariusz Skibicki, ed.), AIP Publishing.

Ranganathan, N., Chalon, F., Meo, S., 2008. Some aspects of the energy based approach to fatigue crack propagation. International Journal of Fatigue 30, 1921-1928.

Ikeda, S., Izumi, Y., Fine, M.E., 1977. Plastic work during fatigue crack propagation in a high strength low alloy steel and in 7050 Al alloy. Engineering Fracture Mechanics 9, 123-128.

Carrascal, I., Casado, J.A., Diego, S., Lacalle, R., Cicero, S., Álvarez, J.A., 2014. Determination of the Paris' law constants by means of infrared thermographic techniques. Polymer Testing 40, 39-45.

Cui, Z.Q., Yang, H.W., Wang, W.X., Yan, Z.F., Ma, Z.Z., Xu, B.S., Xu, H.Y., 2015. Research on fatigue crack growth beahavior of AZ31B magnesium alloy electron beam welded joints based on temperature distribution around the crack tip. Engineering Fracture Mechanics 133, 14-23.

Meneghetti, G., 2007. Analysis of the fatigue strength of a stainless steel based on the energy dissipation. International Journal of Fatigue 29, 81-94.

Ancona, F., Palumbo, D., De Finis, R., Demelio, G.P., Galietti, U., 2016. Automatic procedure for evaluating the Paris Law of martensitic and austenitic stainless steels by means of thermal methods. Engineering Fracture Mechanics 163, 206-219.

Palumbo, D., De Finis, R., Ancona, F., Galietti, U., 2017. Damage monitoring in fracture mechanics by evaluation of the heat dissipated in the cyclic plastic zone ahead of the crack tip with thermal measurements. Engineering Fracture Mechanics 181, 65-75.

Meneghetti, G., Ricotta, M., 2016. Evaluating the heat energy dissipated in a small volume surrounding the tip of a fatigue crack 92 (2), 605-615.

Palumbo, D., Galietti, U., 2017. Thermoelastic Phase Analysis (TPA): a new method for fatigue behaviour analysis of steels. Fatigue & Fracture of Engineering Materials & Structures 4, 523-534.

De Finis, R., Palumbo, D., Galietti, U., 2019. A multianalysis thermography-based approach for fatigue and damage investigation of ASTM A182 F6NM steel at two stress ratios. Fatigue and Fracture of Engineering Materials and Structures 42(1), 267-283.

Dulieu-Barton, J.M., 1999. Introduction to thermoelastic stress analysis. Strain 35, 35–39.

Pitarresi, G., Patterson, E.A., 2003. A review of the general theory of thermoelastic stress analysis. The Journal of Strain Analysis for Engineering Design 38(5), 405–417.
Wang, W.J., Dulieu-Barton, J.M., Li, Q., 2010. Assessment of non-adiabatic behaviour in thermoelastic stress analysis of small scale components. Experimental Mechanics 50, 449–461.
Harwood, N., Cummings, W.M., 1991. Thermoelastic Stress Analysis, Adam Hilger, Bristol Philadelphia and New York.
Stanley, P., 1997. Applications and potential of thermoelastic stress analysis. Journal of Materials Processing Technology 64, 359-370.
Dunn, S.A., 1997. Using Nonlinearities for Improved Stress Analysis by Thermoelastic Techniques. Appl. Mech. Rev. 50(9), 499-513.
Dulieu-Smith, S.M., 1995. Alternative calibration techniques for quantitative thermoelastic stress analysis. Strain 31, 9-16.
Tomlinson, R.A., Olden, E.J., 1999. Thermoelasticity for the analysis of crack tip stress fields – a review. Strain 35, 49-55.
Tomlinson, R.A., Patterson, E.A., 2011. Examination of Crack Tip Plasticity Using Thermoelastic Stress Analysis. Thermomechanics and Infra-Red Imaging. In: Proceedings of the Society for Experimental Mechanics Series, Volume 7, pp 123-129.
Diaz, F.A., Patterson, E.A., Tomlinson, R.A., Yates, R.A., 2004. Measuring stress intensity factors during fatigue crack growth using thermoelasticity. Fracture of Engineering Materials and Structures 27(7), 571–583.
Diaz, F.A., Patterson, E.A., Yates, R.A., 2004. Some improvements in the analysis of fatigue cracks using thermoelasticity. International Journal of Fatigue 26(4), 365–376.
Ancona, F., De Finis, R., Palumbo, D., Galietti, U., 2015. Crack Growth Monitoring in Stainless Steels by Means of TSA Technique. Procedia Engineering 109, 89-96.
Tomei, R., 1981. Criteri di scelta degli acciai inossidabili in funzione degli impieghi. La meccanica italiana, 147.
IRTA™ Manual, 2015. Diagnostic Engineering Solutions (DES srl).